Mon. Not. R. Astron. Soc. **324,** 628–634 (2001)

# The blazar GB 1428+4217: a warm absorber at $z = 4.72$?

A. C. Fabian,[1] A. Celotti,[2★] K. Iwasawa[1] and G. Ghisellini[3]
[1]*Institute of Astronomy, Madingley Road, Cambridge CB3 0HA*
[2]*SISSA, via Beirut, 2-4, 34014 Trieste, Italy*
[3]*Osservatorio Astronomico di Brera-Merate, via Bianchi 46, 23807 Merate (LC), Italy*

Accepted 2001 January 16. Received 2000 December 29; in original form 2000 May 31

**ABSTRACT**

*BeppoSAX* observations of the high-redshift ($z = 4.72$) blazar GB 1428+4217 confirm the presence of a complex soft X-ray spectrum first seen with the *ROSAT* PSPC. Flattening below a rest-frame energy of 5 keV can be accounted for by absorption from an equivalent column density of (cold) gas with $N_{\rm H} \sim 8 \times 10^{22}\,{\rm cm}^{-2}$. Below 2 keV a (variable) excess of a factor of $\sim$20 above the extrapolated absorbed spectrum is also detected. These findings are consistent with and extend to higher redshifts the correlation between increasing soft X-ray flattening and increasing $z$, previously pointed out for large samples of radio-loud quasars. We propose that such features, including X-ray absorption and soft excess emission as well as absorption in the optical spectra, can be satisfactorily accounted for by the presence of a highly ionized nuclear absorber with column $N_{\rm H} \sim 10^{23}\,{\rm cm}^{-2}$, with properties possibly related to the conditions in the nuclear regions of the host galaxy. High-energy X-ray emission consistent with the extrapolation of the medium-energy spectrum is detected up to $\sim$300 keV (rest frame).

**Key words:** galaxies: active – galaxies: individual: GB 1428+4217 – X-rays: galaxies.

## 1 INTRODUCTION

High-redshift active galactic nuclei (AGN) are powerful tools with which to study the physical and cosmological evolution of massive black holes and their relationship with their host galaxies. A particularly interesting class is formed by several high-redshift ($z > 4$), X-ray-bright, radio-loud quasars (Fabian et al. 1997, 1998; Moran & Helfand 1997; Zickgraf et al. 1997; Hook & McMahon 1998), which present characteristics typical of blazars. Interestingly, their X-ray spectra have recently been found systematically to show the presence of spectral flattening in the soft X-ray band. In GB 1428+4217 (Boller et al. 2000), RXJ 1028.6−0844 (Yuan et al. 2000) and PMN 0525−3443 (Fabian et al. 2001), such flattening implies, if interpreted as due to intrinsic X-ray absorption by cold gas, column densities of $1.5 \times 10^{22}$, $2.1 \times 10^{23}$ and $1.8 \times 10^{23}\,{\rm cm}^{-2}$, respectively. These results appear to extend to higher redshift the trend already found in nearer (up to $z = 4.2$) radio-loud quasars observed by *ASCA* and *ROSAT* (Cappi et al. 1997; Fiore et al. 1998; Reeves & Turner 2000), the origin of which is still unclear.

In particular for the most distant object, GB 1428+4217 at $z = 4.72$, previous observations in the X-ray and radio bands have convincingly shown that this AGN is indeed a blazar (Fabian et al. 1997, 1998). Its spectral energy distribution (SED) appears similar to, although more extreme than, those of lower-redshift blazars of similar power, and no strong evidence for different nuclear or jet conditions has been found.

Here we present the results of *BeppoSAX* observations of this source. They were in particular focused on: (a) determining the amount and shape of the flattening and thus its nature, as the MECS allows a good determination of the medium-energy X-ray spectrum; and (b) the detection of the high-energy PDS component, which constrains the position of the $\gamma$-ray (inverse Compton) peak, which for GB 1428+4217 is predicted – by current models – to be at or below $\sim$ MeV.

In the next section we present the analysis and results of the *BeppoSAX* data, which are then discussed in Section 3.

## 2 *BEPPOSAX* DATA

GB 1428+4217 was observed by *BeppoSAX* on 1999 February 4–7 (see Table 1). Signal has been detected in all three main instruments, the two imaging instruments (LECS and MECS) and the PDS one (a collimator), with exposure times of 27.3 (LECS), 90.3 (MECS) and 46.0 (PDS) ks.

A fit over the 1–10 keV band with a simple power law statistically agrees with the previous *ASCA* results (Fabian et al. 1997), both in spectral slope and in absolute flux. No evidence has been found of spectral features associated with Fe emission at about $\sim$1 keV. However, *BeppoSAX* data provide us with interesting information at both the lower and higher energies.

★E-mail: celotti@sissa.it

### 2.1 Low-energy spectrum

The extrapolation of such a power law below 1 keV (and down to 0.4 keV) is well above the data, thus indicating either absorption in excess of the Galactic one (column density $N_{\rm H} = 1.4 \times 10^{20}\,{\rm cm}^{-2}$) or an intrinsic flattening of the spectrum (see Fig. 1). In Table 2 we report the results of the best fits with such additional components: if intrinsic to the source, the corresponding column density is $\sim 7.8 \times 10^{22}\,{\rm cm}^{-2}$. Errors are at the 90 per cent confidence level for one parameter. The quality of the data does not allow us to distinguish statistically between these two possibilities. The spectral slope and intensity are marginally consistent (at $2\sigma$) with those inferred from the *ASCA* and *ROSAT* data (Fabian et al. 1997; Boller et al. 2000).

Below 0.4 keV, however, there appears to be an excess above the model (see Fig. 1). As this might be due to residuals in the background subtraction, we performed a more careful analysis and in particular re-extracted the spectrum by considering the local background. The low-energy excess is still present at the $2\sigma$ level and we therefore consider it, with reasonable probability, to be a real feature. This emission has not been detected in the *ROSAT* data, taken $\sim$2 months previously, suggesting that this component might be variable on intrinsic time-scales of $\sim$10 d. Note that (marginal) indications of variability were also present during the *ROSAT* observation itself (Boller et al. 2000).

### 2.2 PDS data

A strong signal has been also detected in the PDS band. The flux, however, is well above the extrapolation of the LECS+MECS power law (see Fig. 2). We thus checked for possible contamination in the PDS field of view, and indeed found the presence of the BL Lac object 1ES 1426+428 which, fortuitously, had been observed by *SAX* four days after GB 1428+4217 (see Table 1). In collaboration with the 1ES 1426+428 proposing team, we thus tried to disentangle the contributions of the two sources in the PDS.

The spectrum of 1ES 1426+428 is also well described by a power law below 10 keV (Costamante et al. 2001), with a photon index steeper than that of GB 1428+4217, $\Gamma \sim 1.93$. The two observed PDS spectra are, however, very similar and significantly flatter than 1.9 (the data from the 1ES 1426+428 data set are even slightly harder). Therefore this implies either that the dominant contribution in the PDS comes from GB 1428+4217 (assuming its spectrum can be extrapolated from the LECS+MECS power law) or that at higher X-ray energies a flatter component dominates in 1ES 1426+428.

In the former case, a joint spectral fit to the data sets for GB 1428+4217 and 1ES 1426+428 with simple power-law models requires GB 1428+4217 to vary by a factor of $\sim$7 between the two observations, i.e. over a time-scale as short as 2 d, while the high-redshift quasar did not show such strong and fast flux variations in the previous observations (note that they correspond to an intrinsic time-scale of $\sim$8.4 h).

In the second case, the hard PDS spectrum of the 1ES 1426+428 data set is presumed to intrinsically flatten, in a similar manner to that observed in other BL Lac objects (e.g. PKS 2155–304, Chiappetti et al. 1999), with the (flat) inverse Compton component starting to dominate over the (steep) synchrotron one. We then estimated the contribution from 1ES 1426+428 to the PDS data of

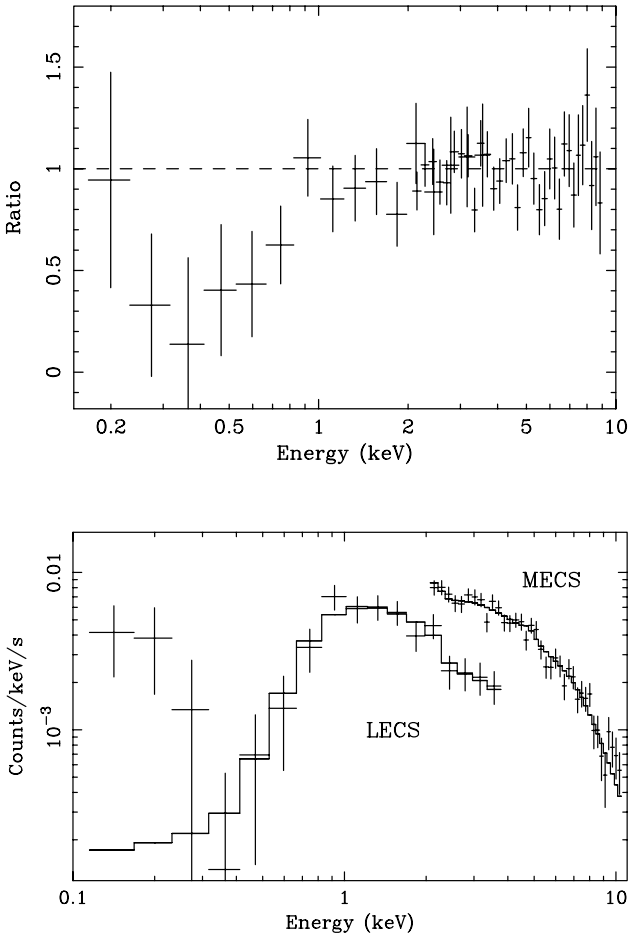


**Figure 1.** The ratio of the data to the absorbed power-law model, after removal of the intrinsic but not the Galactic absorption components (top panel); soft-to-medium X-ray *BeppoSAX* spectrum of GB 1428+4217 fitted over the 1–10 keV band by a power law with cold excess absorption (bottom panel).

**Table 1.** Log of the observations.

| Object | Start time | End time |
|---|---|---|
| GB 1428+4217 | 99-Feb-04 18:04:47 | 99-Feb-07 01:26:40 |
| 1ES 1426+428 | 99-Feb-08 20:48:57 | 99-Feb-09 21:14:39 |

**Table 2.** Results of the spectral fits (0.4–10 keV).

| Model | $N_{\rm H}$ ($10^{22}\,{\rm cm}^{-2}$) | $\Gamma_1$ | $E_{\rm break,obs}$ (keV) | $\Gamma_2$ | $\chi^2$/d.o.f. |
|---|---|---|---|---|---|
| Power law + free intrinsic $N_{\rm H}$ (0.4–10 keV) | $7.8^{+8.7}_{-6.0}$ | $1.45 \pm 0.10$ | – | – | 37.4/47 |
| Broken power law (0.4–10 keV) | $N_{\rm H,gal}$ | $-1.5 \pm 2.5$ | $0.86^{+1.68}_{-0.19}$ | $1.41 \pm 0.09$ | 36.7/46 |

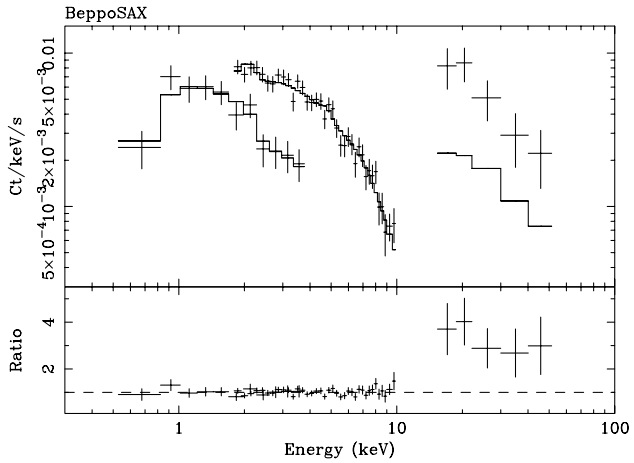


**Figure 2.** The *BeppoSAX* spectrum of GB 1428+4217. The plot shows the best-fitting power-law model to the LECS+MECS data. The surplus emission in the PDS band is probably due to contamination from 1ES 1426+428.

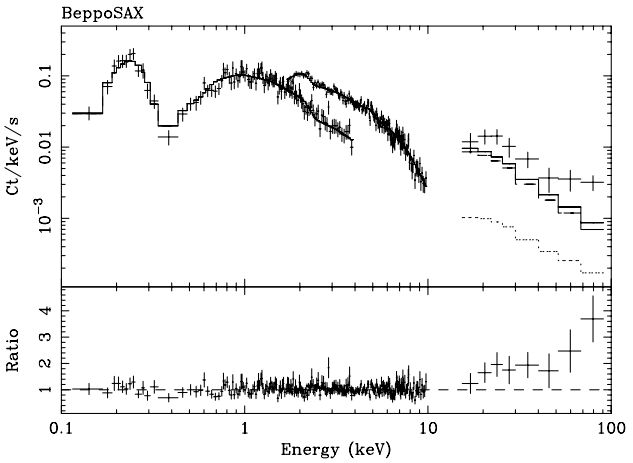


**Figure 3.** The spectrum of 1ES 1426+428 with the best-fitting power-law model to the LECS+MECS data. The contribution expected from GB 1428+4217 in the PDS band has been taken into account (dotted line). There is still surplus emission in the PDS band, which is probably due to the BL Lac object itself, unless GB 1428+4217 brightened by a factor of ∼7 since it was observed with *BeppoSAX* two days previously.

the GB 1428+4217 observation iteratively, by assuming that the fluxes from the two sources are constant between the observations and that the spectrum of GB 1428+4217 is a single power law across the *BeppoSAX* energy range (from 0.5 to 100 keV). Uncertainties in the relative normalization factors between PDS and MECS are a problem: in order to reduce the number of free parameters, and for consistency with the assumption of constant fluxes, we fixed these factors to 0.8 for both data sets.

Fig. 3 shows the 1ES 1426+428 data with the best-fitting power-law model for the LECS+MECS data extrapolated to the PDS energy range, and with a contribution from GB 1428+4217 derived from its spectral fit (as in Fig. 2).[1] Excess flux is still present in the PDS band. The surplus emission is attributed to a flat spectral component emerging above 10 keV from 1ES 1426+428; that is, the entire broad-band spectrum of the BL Lac is represented by a broken power law. Once the estimated contribution from GB 1428+4217 ($\Gamma = 1.45 \pm 0.10$) is added, this model gives a good fit to the data ($\chi^2 = 242.2$ for 263 d.o.f.; see Fig. 4). Photon indices below and above the break energy of 9.26 keV are $\Gamma_1 \simeq 1.93$ and $\Gamma_2 \simeq 1.34$, respectively. The corresponding spectrum for GB 1428+4217 is well fitted with a single power law ($\chi^2 = 40.8$ for 54 d.o.f.; Fig. 5). Although the contribution from 1ES 1426+428 may be slightly overestimated (see the residuals in the PDS band in Fig. 5), the PDS data in the GB 1428+4217 observation appear to be dominated by the contamination from 1ES 1426+428.

The observer-frame 2–10 keV fluxes for the two sources are $2.76 \times 10^{-12}$ erg cm$^{-2}$ s$^{-1}$ for GB 1428+4217, and $2.0 \times 10^{-11}$ erg cm$^{-2}$ s$^{-1}$ for 1ES 1426+428 (compatible with the results from the *ASCA* observation of 1994 February 6 by Kubo et al. 1998). The 20–100 keV fluxes are $1.1 \times 10^{-11}$ and $6.3 \times 10^{-11}$ erg cm$^{-2}$ s$^{-1}$ for GB 1428+4217 and 1ES 1426+428, respectively.

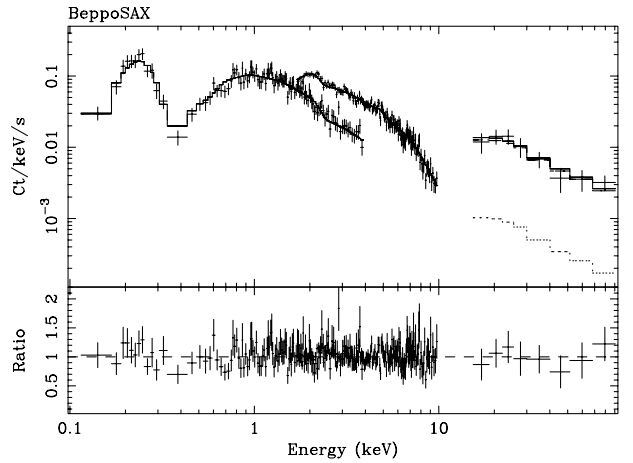


**Figure 4.** The spectrum of 1ES 1426+428 fitted with a broken power-law model. The plot shows the best-fitting model including the contribution from GB 1428+4217 (see the legend of the previous figure).

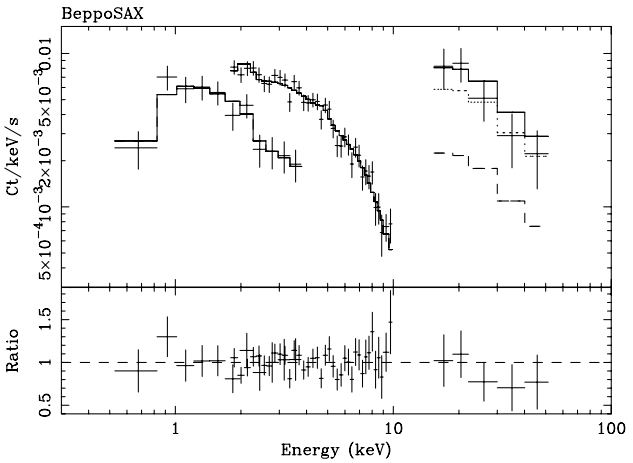


**Figure 5.** The spectrum of GB 1428+4217 fitted with a power-law model including the contribution from 1ES 1426+428 (dotted line) which is based on the broken power-law fit (see previous figure). The contribution from the BL Lac object appears to dominate the detected PDS counts above 20 keV.

## 3 DISCUSSION

We have presented the results of the *BeppoSAX* observations of the most distant radio-loud X-ray-luminous quasar GB 1428+4217.

[1] We adopted a transmission efficiency of 46 per cent in the PDS field of view during the 1ES 1426+428 observation.

This has allowed us to study and reveal interesting features at the extremes of the *BeppoSAX* X-ray-energy window.

At the higher-energy end of the *BeppoSAX* broad-band spectrum, the contamination of the PDS data from 1E1426+428 unfortunately does not allow us to determine the spectrum of GB 1428+4217 with sufficient accuracy to constrain any curvature which might indicate the position of the high-energy $\gamma$-ray peak. However, from the decontamination we performed, the spectrum appears consistently to extend to the higher detected intrinsic energies, i.e. 280 keV in the blazar rest frame.

### 3.1 Low-energy spectrum

At the lowest energies, $<1$ keV, the *BeppoSAX* observations robustly confirm the presence of the flattening in the spectrum found in the *ROSAT* PSPC spectrum (Boller et al. 2000). In addition, below 0.4 keV emission a factor of $\sim$20 in excess of the flattened spectrum has been found (see Fig. 1).

The origin of the flattening has been discussed in some detail by several authors (Cappi et al. 1997; Fiore et al. 1998; Elvis et al. 1998; Boller et al. 2000; Yuan et al. 2000; Fabian et al. 2001; Reeves & Turner 2000), but no definite conclusion could be drawn. Certainly, the detection of such a feature by a variety of instruments (*ROSAT*, *ASCA*, *BeppoSAX*) argues against any systematic miscalibration effect.

The first interesting point that has been made is that the flattening seems to be associated only with radio-loud objects, therefore suggesting its origin to be intrinsic. The number of good-quality X-ray spectra of radio-quiet quasars at $z > 1.5$ is unfortunately limited. However, the recent results by Vignali et al. (2001), combined with the findings of Reeves & Turner (2000), imply that in only two out of 15 radio-quiet quasars (in the range $z = 1.8$–$2.5$) has a positive detection of flattening corresponding to $N_{\rm H} \sim 10^{22}\,{\rm cm}^{-2}$ been established, despite the biased selection of X-ray-loud sources. For comparison, five out of six radio-loud objects in the same redshift range have equivalent $N_{\rm H} \geq 10^{22}\,{\rm cm}^{-2}$ (see Fig. 6). We therefore favour the possibility that the flattening is due to an intrinsic property of the source, possibly associated with the radio-loudness phenomenon. Nevertheless we note that radio-loud objects tend to be more X-ray-luminous and so yield the best spectra at a given redshift, and therefore in the following we also discuss the possible role of absorption of intergalactic origin.

We consider it unlikely that large- (galactic) scale gas is responsible for the X-ray absorption, given the large masses of gas implied by such a hypothesis as well as the lack of any clear connection with the radio-loud phenomenon. Therefore in the following we concentrate on the nuclear and/or cosmological properties that could account for such a feature.

A further key piece of information is the presence of a systematic trend of the flattening in the spectra of radio-loud quasars to increase with redshift (Cappi et al. 1997; Fiore et al. 1998; Reeves & Turner 2000). The inclusion of the recent results on RXJ 1028.6−0844 (Yuan et al. 2000), PMN 0525−3343 (Fabian et al. 2001) and GB 1428+4217 itself strengthens and extends this behavior up to $z \geq 4.7$, as shown in Fig. 6. Although no correlation between the flattening and other spectral property has previously been found, we stress the possible presence of a significant trend of increasing $N_{\rm H}$ with increasing hard X-ray luminosity (intrinsic 2–10 keV band), as can be argued from Fig. 7. Unfortunately, small statistics do not allow us to disentangle the redshift and luminosity dependences.

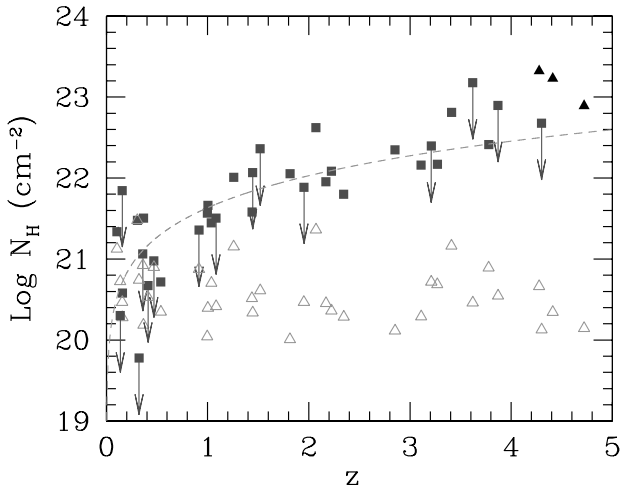


**Figure 6.** Absorption column density – as a measure of the soft X-ray flattening – versus redshift of radio-loud quasars. The data comprise the *ASCA* results reported by Reeves & Turner (2000) (filled squares) and the three sources above $z > 4$ (GB 1428+4217, PMN 0525−3343, RXJ 1028.6−0844, filled triangles). The empty symbols indicate the Galactic column density for each object. The dashed line corresponds to the IGM column density, for $\Omega_0 = 0.3$, $\Omega_{\rm b} = 0.06$ and solar metallicity).

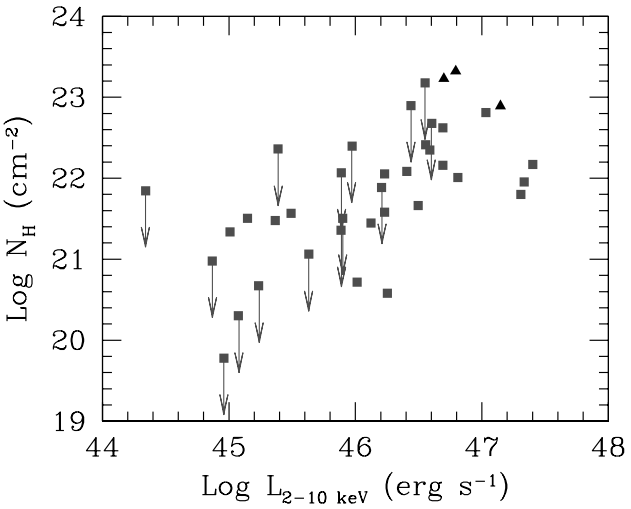


**Figure 7.** Absorption column density – as measure of the soft X-ray flattening – versus hard X-ray luminosity (2–10 keV). Symbols and objects as in Fig. 6.

In Fig. 6 we also show the line-of-sight value of $N_{\rm H}$ due to the intergalactic medium (IGM) assuming solar abundances. If the IGM were enriched by redshifts of about 4 to the same metallicity as clusters of galaxies, the correlation with redshift could be explained. As discussed in the *ROSAT* PSPC work on GB 1428+4217 (Boller et al. 2000) this conclusion does not agree with observations of the metallicity of the Lyman $\alpha$ forest. Only if there were a strong correlation between enrichment and temperature of the IGM phase might some agreement occur, but even then the enrichment requirements would be huge.

A more plausible interpretation of the apparent correlation shown in Fig. 6 would then be that it arises from the detection limit for absorption in present X-ray detectors. For example, a limit of a few times $10^{20}\,{\rm cm}^{-2}$ at $z = 0$ would correspond to a few times $(1+z)^3 10^{20}\,{\rm cm}^{-2}$ at redshift $z$, which roughly scales with the points in Fig. 6.

Let us now examine the alternative hypothesis of an intrinsic origin of the flattening. As discussed by Fabian et al. (2001), on nuclear scales this might arise because of: (a) the characteristic shape of the energy distribution of the particles and/or photons that are believed to be responsible – through inverse Compton scattering on the soft external photon field – for the high-energy spectral component in blazars; or (b) absorption by nuclear, highly ionized gas.

Let us therefore consider in turn how these two possibilities could account for the spectral characteristics discussed so far. These, including the results of the present analysis on GB 1428+4217, can be summarized as follows: a spectral flattening below ~5 keV; soft excess emission below ~2.3 keV; a possible connection with radio-loudness/jets and with the redshift and/or X-ray luminosity; and an optical spectrum showing evidence of absorption features (Ly$\alpha$–N V and C IV) (Hook & McMahon 1998; see Fabian et al. 2001 for the similar case of PMN 0525−3433). We recall that the latter (optical) feature is indeed typically seen in outflows (Brandt, Laor & Wills 2000).

Within scenario (a), which implicitly links the observed properties with blazar-type sources, the flattening could be caused by several effects, such as an intrinsic break in the low-energy part of the non-thermal electron distribution (e.g. caused by incomplete cooling) which would require a break energy of ~few $m_e c^2$; a paucity in the (relative) amount of synchrotron photons that are scattered at higher energies (synchrotron self-Compton emission) and thus typically contribute to the soft-to-medium X-ray band flux, filling the 'depression' between the synchrotron and inverse Compton components in blazars (e.g. Sikora, Begelman & Rees 1994);[2] and the intrinsic flattening of the external soft photon energy distribution below its peak, which translates into a flattening in the scattered inverse Compton component at soft X-ray energies. Furthermore, the presence of a soft X-ray excess, as seen in GB 1428+4217 and RXJ 1028.6−0844 could be consistent with this scenario as due to either Comptonization of a cold electron component in the jet (bulk Compton emission, Sikora et al. 1994) or the high-energy tail of the soft radiation field.

Nevertheless, a serious problem arises with this scenario, if the soft X-ray spectrum is produced by low-energy electrons. In fact, while the uncertainties in the determination of the spectral shape/absorption in the high-redshift objects do not allow the presence of any spectral variation to be found, soft X-ray flux variability has been established for GB 1428+4217 on time-scales of ~1 d (Fabian et al. 1999). Although strong and fast variability is of course expected in blazars, thanks to the enhancement caused by relativistic beaming, the cooling time-scales of electrons emitting at soft X-ray energies – as discussed in scenario (a) – would greatly exceed the observed variability time-scale.

In scenario (b), i.e. absorption by small-scale gas, such as nuclear absorbing winds and outflows, the flattening *and* the soft X-ray excess can be successfully accounted for by the presence of a warm/highly ionized absorber with a column density of the order of $10^{23}\,\mathrm{cm}^{-2}$ and $\xi \sim 10^2$ (where the ionization parameter is defined as $\xi \equiv L/(nR^2)$, with $L$ as the ionizing luminosity from 1 to 1000 Ryd). In Fig. 8 we report the results of the spectral fitting to the *BeppoSAX* data with such a model, as calculated using the photoionization code CLOUDY C90.04 (Ferland et al. 1998). The predicted model spectrum (see Fig. 8) clearly shows the presence of edges at ~1.5 keV (Fe XX–Fe XXIV) and ~0.25–0.3 keV (Mg). Most absorption is due to oxygen. Solar metallicity has been assumed in these nuclear regions. $\chi^2 = 29.2/40$.

We further explored the viability of such a scenario by considering previous observations of GB 1428+4217. In Fig. 9 the contour plots for the two critical parameters of the model – the gas column density and the ionization state – are shown for the *BeppoSAX*, *ASCA* and *ROSAT* PSPC data (Fabian et al. 1997, 1998). A common range of (marginally consistent) parameters, around $\xi \sim$ 600–700 and column densities of $\sim 3 \times 10^{23}\,\mathrm{cm}^{-2}$, can be found for the three data sets. Some of the variation may be due to spectral variability among the observations.

Note that, if this picture is correct, the lack of significant extinction in the optical–UV bands (similar to what is seen in PMN 0525−3433) also requires that the absorbing gas is highly ionized and/or rich in metals and lacking in dust. (The observed intense and fast variability is inconsistent with its being caused by the

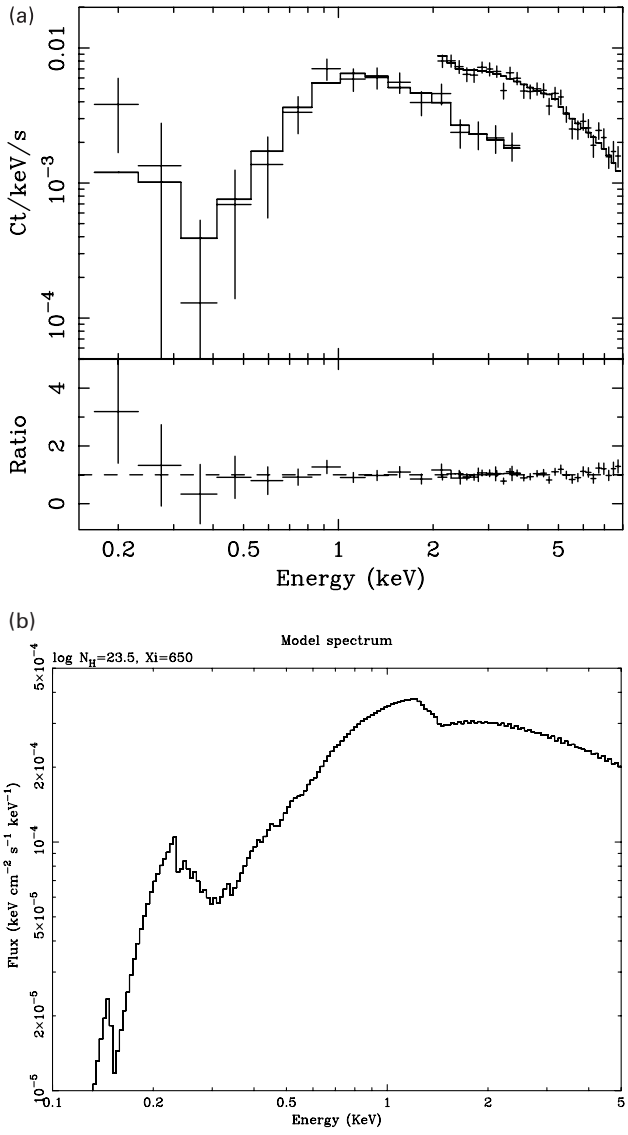


**Figure 8.** (a) Fit with a warm absorber of the *BeppoSAX* data, for a column density $N_{\mathrm{H}} = 10^{23.5}\,\mathrm{cm}^{-2}$ and ionization parameter $\xi = 650$ and (b) the corresponding model. Edges at ~ 1.5 keV (Fe) and ~0.25 (Mg) and 0.3 keV (Si) are clearly visible. Solar metallicity has been assumed.

[2] Note that an increase in the dominance of the external Compton component is naturally associated with an increase in the source X-ray luminosity.

postulated warm absorber itself and therefore has to be ascribed to the primary emission from relativistic plasma.)

The ionization parameter $\xi$, column density $N_{\rm H}$ and luminosity $L$ along our line of sight to GB 1428+4217 require the warm absorber to be located at an estimated distance from the nucleus of less than about 200 pc. The increase of the amount of absorption with redshift, but also with luminosity, argues for an even larger increase in the amount of gas, plausibly associated with a large (super-Eddington) accretion rate of infalling gas in the early stages of nuclear activity, and/or outflows possibly confining powerful radio jets. The warm absorber may also be the inner part of the dense interstellar medium of the young host galaxy (see Fabian 1999 for a more general discussion).

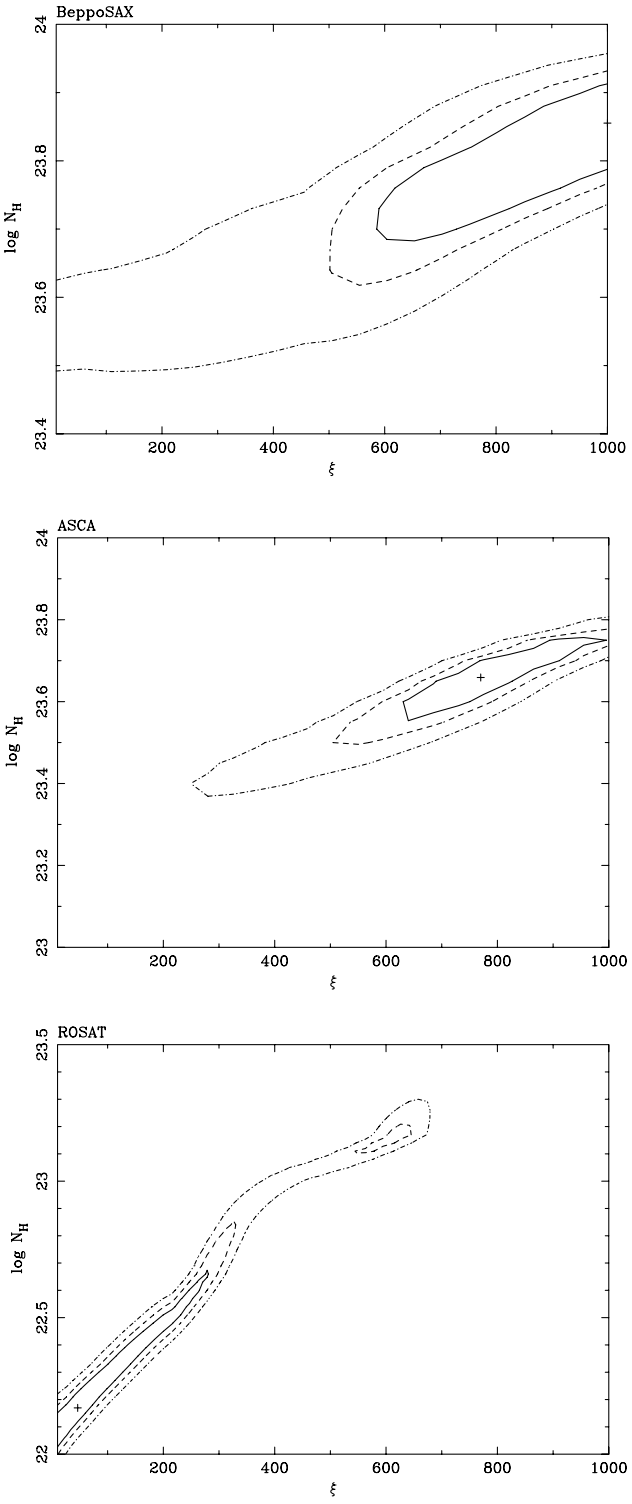


**Figure 9.** Confidence contours for the two parameters $N_{\rm H}$ and $\xi$ describing the warm absorber properties, fitting *BeppoSAX*, *ASCA* and *ROSAT* data of GB 1428+4217 (see references in the text). A (marginally) consistent solution describing all three data sets can be found around $N_{\rm H} = 10^{23.3–23.5}\,{\rm cm}^{-2}$ and $\xi \sim 600–700$.

If this gas completely envelops the source then its mass is $\sim 10^9 r_{200}^2\,{\rm M}_\odot$, where the radius is $200 r_{200}$ pc. It is possible that in directions well away from the axis of the blazar jet, the surrounding gas is of low ionization and so opaque to all but hard X-rays, and that only in the jet direction is the X-ray intensity powerful enough to ionize the gas. Therefore in more extreme, high-$z$ sources, such gas might completely hide the presence of activity in the soft-to-medium X-ray band. Moreover, under such conditions of high optical depths, the nuclear disc radiation might be partly reflected back by the gas, thus enhancing the nuclear radiation energy density. The high amount of scattering gas should also allow significant detection of nuclear emission in the most powerful radio galaxies.

The decrease in absorption seen in objects below a redshift of $\sim$1 (see Fig. 6) may be associated with this gas being consumed by star formation, or having been blown out of the host by a quasar wind. The predominance of absorption in radio-loud objects could be related to their having more massive host galaxies (and thus it being more difficult to blow the gas away) and/or to the radio phase being associated with the quasar youth.

Observations of GB 1428+4217 and similar high-redshift blazars with high sensitivity and energy resolution instruments, such as those provided by XMM, will soon allow us to determine whether these conditions are ubiquitous in high-$z$ sources. They should robustly test the proposed warm absorber scenario by detecting the edges predicted in Fig. 8 and so enable us to infer the physical conditions in the active nuclear regions of primeval galaxies.

## ACKNOWLEDGMENTS

We thank Gary Ferland for the use of his code CLOUDY. The Royal Society (ACF) and the Italian MURST and ASI grant ARS-99-74 (AC) are thanked for financial support.

## REFERENCES

Boller Th., Fabian A. C., Brandt W. N., Freyberg M. J., 2000, MNRAS, 315, L23
Brandt W. N., Laor A., Wills B., 2000, ApJ, 528, 637
Cappi M., Matsuoka M., Comastri A., Brinkmann W., Elvis M., Palumbo G. G. C., Vignali C., 1997, ApJ, 478, 492
Chiappetti L. et al., 1999, ApJ, 521, 552
Costamante L. et al., 2001, A&A, in press
Elvis M., Fiore F., Giommi P., Padovani P., 1998, ApJ, 492, 91
Fabian A. C., 1999, MNRAS, 308, L39
Fabian A. C., Brandt W. N., McMahon R. G., Hook I., 1997, MNRAS, 291, L5
Fabian A. C., Iwasawa K., McMahon R. G., Celotti A., Brandt W. N., Hook I. M., 1998, MNRAS, 295, L25
Fabian A. C., Celotti A., Iwasawa K., Carilli C. L., McMahon R. G., Brandt N. W., Ghisellini G., Hook I. M., 2001, MNRAS, 323, 373
Fabian A. C., Celotti A., Pooley G., Iwasawa K., Brandt N. W., McMahon R. G., Hoenig M. D., 2000, MNRAS, 308, L6

Ferland G. J., Korista K. T., Verner D. A., Ferguson J. W., Kingdon J. B., Verner E. M., 1998, PASP, 110, 761
Fiore F., Elvis M., Giommi P., Padovani P., 1998, ApJ, 492, 79
Hook I., McMahon R. G., 1998, MNRAS, 294, L7
Kubo H., Takahashi T., Madejski G., Tashiro M., Makino F., Inoue S., Takahara F., 1998, ApJ, 504, 693
Moran E. C., Helfand D. J., 1997, ApJ, 484, L95
Reeves J. N., Turner M. J. L., 2000, MNRAS, 316, 234
Sikora M., Begelman M., Rees M. J., 1994, ApJ, 421, 153
Vignali C., Comastri A., Cappi M., Palumbo G. G. C., Matsuoka M., 2001, Adv. Space Res., 25, 861
Yuan W., Matsuoka M., Wang T., Ueno S., Kubo H., Mihara T., 2000, ApJ, 545, 625
Zickgraf F.-J., Voges W., Krautter J., Thiering I., Appenzeller I., Mujica R., Serrano A., 1997, A&A, 323, L21

This paper has been typeset from a TEX/LATEX file prepared by the author.